ACS Chemical Neuroscience

Letter

pubs.acs.org/chemneuro

Interaction between Amyloid-β Peptide and Heme Probed by Electrochemistry and Atomic Force Microscopy

Yanli Zhou, Jing Wang, Lantao Liu,* Rongrong Wang, Xinhe Lai, and Maotian Xu*

Henan University Key Laboratory of Nanobiological Analytical Chemistry, Department of Chemistry and Chemical Engineering, Shangqiu Normal University, Shangqiu 476000, China

Supporting Information

ABSTRACT: Heme binds to amyloid β-peptide (Aβ) in the brain of Alzheimer's disease (AD) patients, thus forming Aβ-heme complexes and leading the characteristic pathological features of AD. The interaction between heme and Aβ might have important biological relevance to AD etiology. In this work, the electrochemical performances of heme after incubation with Aβ1−42, Aβ fragments, and mutated Aβ were systematically investigated using cyclic voltammetry and differential pulse voltammetry. Our results indicated that His13 and His14 were possible binding sites, and Aβ bound two molecules of heme with a binding constant of $K_{a1} = 7.27 \times 10^6$ M^{-1} ($n_1 = 1.5$) and $K_{a2} = 2.89 \times 10^6$ M^{-1} ($n_1 = 1.8$). Detailed analysis with atomic force microscopy (AFM) of Aβ1−42 in the absence or presence of heme under the same incubation conditions showed that heme inhibited the formation of Aβ fibrils. According to results of the spectroscopic characterization, Arg5 was the key residue in making the heme-Aβ1−42 complex as a peroxidase.

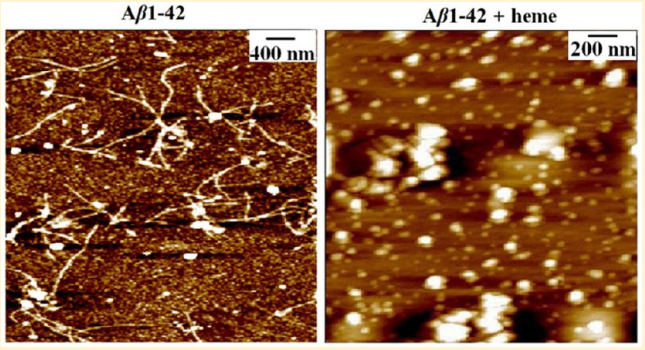

KEYWORDS: *Amyloid β-peptide, heme, interaction, electrochemical method, atomic force microscopy, UV−vis spectroscopy*

Alzheimer's disease (AD) is one of the most common progressive neurodegenerative diseases and has an incidence rising almost logarithmically with age.[1−3] It has become a very serious healthy and social problem with the general life-expectancy gradually increasing. Although not fully understood, many studies have demonstrated that the disease is caused by deposits in the brain tissues of amyloid β-peptide (Aβ).[4−10] Aβ appears prevailingly in two forms: Aβ1−40 and Aβ1−42, while the latter has two more residues at the C-terminus. The role of metal ions (Cu^{2+}, Fe^{3+}, and Zn^{2+}) in modulating the Aβ aggregation and in generating reactive oxygen species (ROS) has attracted increasing attention due to the fact that abnormally high concentrations of metal ions exist within senile plaques.[11−15] Fe^{3+} as a redox-active metal ion is a facilitator of oxidative stress by the production of hydroxyl radicals from H_2O_2 via the Fenton reaction.[16] In the brain, Fe^{3+} is mainly associated with ferritin and relatively very low levels are free ions. Moreover, the Fe^{3+} chelation has been reported to be protective for Aβ aggregation.[16]

Heme, which is essential to the function of a number of proteins, is a ferroprotoporphyrin IX complex. Recent studies demonstrate that heme concentration is abnormal in brain of AD patients compared with controls.[17,18] Heme binds to Aβ to form an Aβ-heme complex, and the Aβ aggregation can be prevented. Depletion of regulatory heme by Aβ induces synthesis of heme, uptake of iron, abnormal iron homeostasis, and decay of iron regulatory proteins in human neuroblastoma cells. The Aβ-heme complex also shows peroxidase activity and catalyzes the oxidation of serotonin and 3,4-dihydroxyphenylalanine by H_2O_2. The peroxidase activity leads to the oxidative damage and the decline in specific neurotransmitters. The above symptoms are the characteristic pathological features of AD, and thus study of the Aβ-heme complex may open a new direction for the research of AD.

Using circular dichroism spectroscopy, Tan and co-workers reported that Aβ-heme complex could stabilize the α-helix structure of Aβ1−40 to inhibit Aβ1−40 aggregation.[19] Atamna et al. compared heme-binding between human Aβ and rodent Aβ by the use of UV−vis and fluorescence spectroscopy.[20] They concluded that human Aβ bound heme with higher affinity than rodent Aβ, and three amino acids including Arg5, Tyr10, and His13 played important role in heme-binding of human Aβ. However, regarding the heme-binding sites, conflicting results were reported. Dey's group used wild-type and mutated Aβ to investigate their interaction with heme by UV−vis spectroscopy.[21] Their results showed that His13 and His14 residues were the heme-binding ligands and Arg5 residue served as the proton source required for peroxidase activity of Aβ-heme complex. Therefore, the specific mechanism of heme in AD needs further research.

Received: December 19, 2012
Accepted: January 21, 2013
Published: January 21, 2013

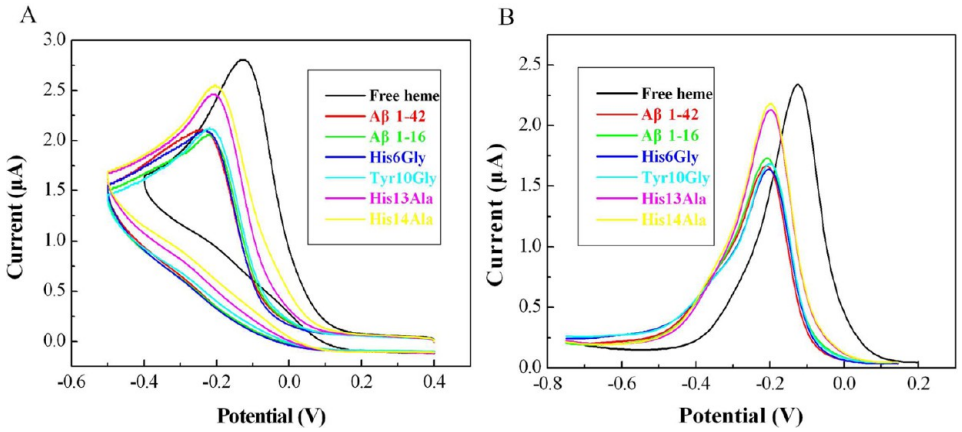

Figure 1. CV (A) and DPV (B) of 5 μM heme incubated with 5 μM Aβ in 0.1 M PBS (pH 7.4): free heme, black; Aβ1−42, red; Aβ1−16, green; His6Gly, blue; Tyr10Gly, cyan; His13Ala, magenta; His14Ala, yellow.

Heme has good electrochemical activity, and electrochemical methods can allow for accurate and direct determination of potentials of redox-active biomolecules. Electrochemical investigations are expected to provide a model for the mechanistic study of electron exchange between heme and Aβ. In addition, atomic force microscopy (AFM) is a tool of undeniable value for the study of biologically relevant samples due to its potential to image the structure of biomolecules with molecular (or even submolecular) resolution.[22] One can carry out measures under physiological conditions with AFM, which minimizes the damages in the soft biomaterials under tapping mode. Reports have used AFM to monitor the influence of metal ions including Fe^{3+}, Cu^{2+}, and Zn^{2+} on the deposition and aggregation of Aβ on a solid template.[23,24] However, to our knowledge, few reports exist on the AFM study of effects of heme binding in the Aβ aggregation process. Thus, the role of heme in modulating the Aβ aggregation characterized by AFM would be of great interest.

Keeping this aim in view, we used electrochemical method and AFM characterization to explore the interaction of Aβ and heme including the binding sites, binding constant, number of binding sites, and effect of aggregation. The peroxidase actitivity of heme-Aβ1−42 complex was also investigated by UV−vis spectroscopy.

RESULTS AND DISCUSSION

Binding Residues. It is generally accepted that heme binds to the hydrophilic portion of Aβ species (residues 1−16) and the possible binding ligands are His6, His13, His14, and Tyr10. Thus, Aβ1−42 and Aβ1−16 fragment have been used, and site-directed mutants of Aβ1−16 including His6Gly, His13Ala, His14Ala, and Tyr10Gly have been selected to investigate the effect of elimination of the possible positions individually. Voltammetry is a rapid and convenient technique to determine subtle changes in redox properties of the electroactive species reflecting their interactions, and is used in this study. Figure 1 is an overlay of the cyclic voltammetry (CV) and differential pulse voltammetry (DPV) of equal heme incubated with the above Aβ peptides. Utilization of the two voltammetry generated similar results. For free heme (black curve), a well-defined reduction peak location at −0.12 V was observed, indicating that heme had a good reduction activity. After incubation with Aβ peptides, oxidation state of heme in the complex was preserved upon binding to Aβ and could be chemically reduced. The reduction peak potential shifted from −0.12 V to about −0.20 V. The negatively shifted reduction potential demonstrated that heme after incubation with Aβ was more difficult to be reduced. Meanwhile, the reduction peak current of heme in the presence of Aβ peptides decreased remarkably. Together, the above results indicated that the heme bound Aβ in complex form,[17] and the conformational changes diminished the amount of heme to the electrode surface.

The similar changes of the voltammetric curves for both of Aβ1−42 (red) and Aβ1−16 (green) proved that the binding sites of heme-Aβ complex lay within the 1−16 peptide sequence. The single mutant His6Gly (blue) and Tyr10Gly (cyan) bound heme like native Aβ1−42 as reflected from the voltammetric curves, indicating that neither of them was coordinating residue. Compared with Aβ1−42, the reduction peak current of the single mutant His13Ala (magenta) and His14Ala (yellow) increased to some extent, implying that the elimination of His13 and His14 weakened the coordination of heme with Aβ. Therefore, His13 and His14 were the binding sites of heme-Aβ complex.[21]

Binding Constant and Number of Binding Sites. The binding of the heme with Aβ1−42 could be quantitatively analyzed by the number of binding sites (n) and the apparent association constant (K_a). Fixed concentration of Aβ1−42 was mixed with increasing concentrations of heme. To ensure the binding equilibrium, heme and Aβ1−42 were incubated at 37 °C for 1 h, even though the interaction was rapid.[20] Centrifugation was used to separate the bound heme in complex form from the unbound heme, because Aβ1−42 and heme-Aβ1−42 complex could be removed by high speed centrifugation. The concentration of free heme, which referred to the concentration of unbound heme at the end of the 1 h incubation of 5 μM Aβ1−42, was obtained from the calibration plot of reduction peak current versus concentration of heme (Figures S1 and S2, Supporting Information). The concentration of the bound heme could be further calculated by subtracting the free heme from the total heme (Table S1, Supporting Information). For the equilibrium system, the binding sites might be calculated according to the Scatchard model when the binding was single receptor population. A curved Scatchard plot would be obtained, if the binding had more than one type of site. [25] The Scatchard plot is defined by eqs 1 and 2:

dx.doi.org/10.1021/cn300231q | ACS Chem. Neurosci. 2013, 4, 535−539

$$\frac{r}{C_f} = nK_a - K_a r \quad (1)$$

$$r = \frac{C_b}{C_p} \quad (2)$$

where r represents the number of moles of bound heme (C_b) per mole of Aβ, n can represent the number of binding sites on the Aβ1−42 molecule, K_a is the association constant, C_f is the concentration of free heme, and C_p is the total concentration of Aβ1−42.

Figure 2 shows the Scatchard plot of the interaction between heme with Aβ1−42. The Scatchard plot has two regression

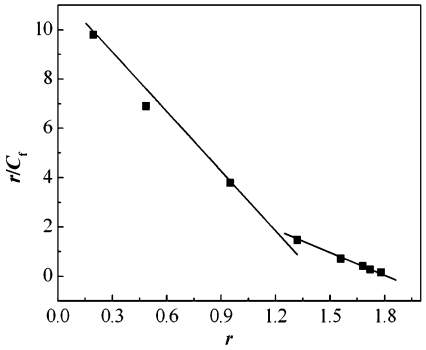

Figure 2. Scatchard plot of the interaction between heme with Aβ1−42. [Aβ1−42] = 5 μM, $[\text{heme}]_{total}$ = 1, 2.5, 5, 7.5, 10, 12.5, 15, and 20 μM.

curves, reflecting that Aβ1−42 bound two molecules of heme.[26] From these plots, the binding parameters of K_a and n for the binding of heme with Aβ1−42 could be easily calculated using eq 1. For the two molecules binding, $K_{a1} = 7.27 \times 10^6$ M^{-1}, n_1 = 1.5 and $K_{a2} = 2.89 \times 10^6$ M^{-1}, n_2 = 1.8 were obtained. The value of n was approximate to 2, which was consistent with the result of the His13 and His14 as the binding sites of heme-Aβ complex. Moreover, the K_{a2} was lower than K_{a1}, suggesting that the binding of first heme molecule had high affinity at low concentration, while the second heme molecule bound Aβ with low binding affinity and selectivity at high concentration.

Effect of Heme on Aβ Aggregate Formation. The effect of heme on Aβ1−42 aggregate formation on mica slides were investigated by the AFM characterization. Images obtained from AFM topographs of aliquots of Aβ1−42 in the presence or absence of heme taken at different incubation times are shown in Figure 3. As expected, just a few Aβ1−42 oligomers with a height of 1−2 nm appeared at the beginning of incubation without (Figure 3A) or with heme (Figure 3F). As time elapsed (~12 h), oligomers agglomerated into larger globular aggregates in the absence of heme (Figure 3B). As a comparison, the coexistence of oligomers and amorphous aggregates were observed in the presence of heme (Figure 3G). The height of these globular and amorphous aggregates ranged from 2 to 5 nm, and the diameters were 10−80 nm. After 36 h incubation at 37 °C, most of the globular aggregates in the absence of heme appeared to be converted into protofibrils with heights of 2−7 nm and lengths up to 800 nm (Figure 3C), while a large number of amorphous aggregates appeared in the presence of heme (Figure 3H). When the incubation was prolonged to 72 h, the heme-free Aβ1−42 solution produced fibrils with the length of 1−2 μm (Figure 3D). The cursor profile for the line indicated that the heights of fibrils were about 6 nm (Figure 3E). This was in sharp contrast to the heme-containing solution in which the amorphous aggregates became larger and more abundant (Figure 3I and J). These observations suggest that the interaction of heme with Aβ1−42 may inhibit the formation of amyloid aggregates in fibrillar form.

To further verify the above observation, the effect of heme concentration on the Aβ1−42 aggregation was explored. The solution of Aβ1−42 monomers was incubated with heme at different concentrations at 37 °C for 24 h. The AFM results are shown in Figure 4. The total amount of aggregates decreased with the decreasing concentration of heme in the incubation solution, indicating that heme could inhibit Aβ1−42 aggregation. The results were consistent with findings reported by Atamna and Boyle[18,27] Heme prevented the aggregation of

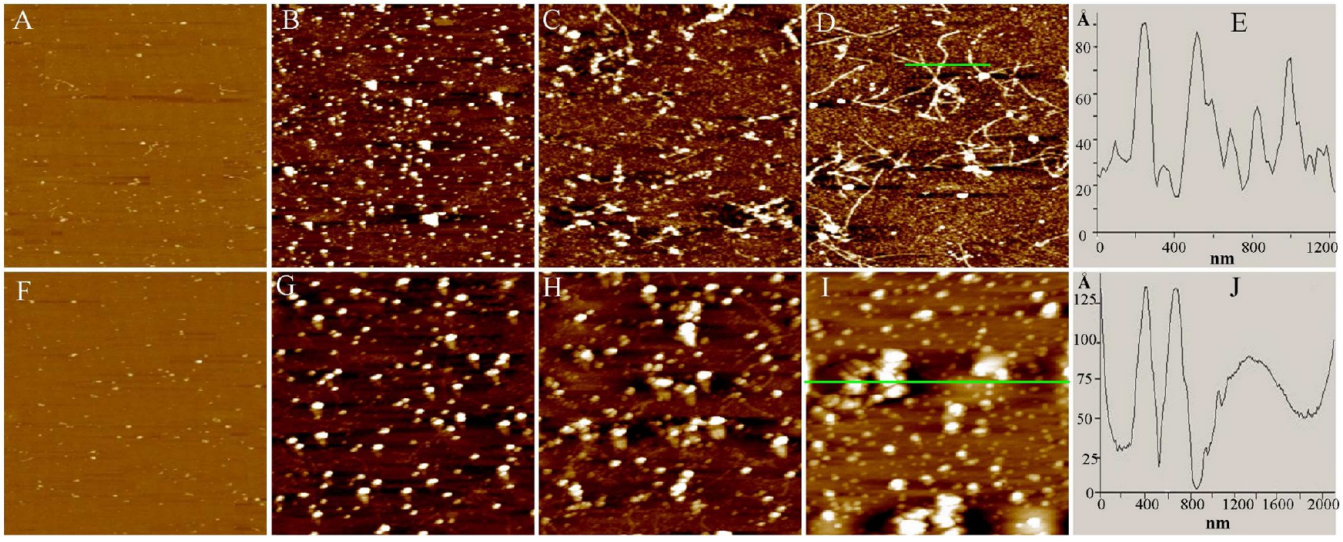

Figure 3. AFM images of 1 μM Aβ1−42 aggregates formed in 0.1 M PBS (pH 7.4) incubated at 37 °C in the absence (A−D, 4 μm × 4 μm) or presence (F−I, 2 μm × 2 μm) of 1 μM heme for different times: (A, F) 0 h, (B, G) 12 h, (C, H) 36 h, and (D, I) 72 h. (E) and (J) are the representative cursor profile for the line in (D) and (I), respectively.

dx.doi.org/10.1021/cn300231q | ACS Chem. Neurosci. 2013, 4, 535−539

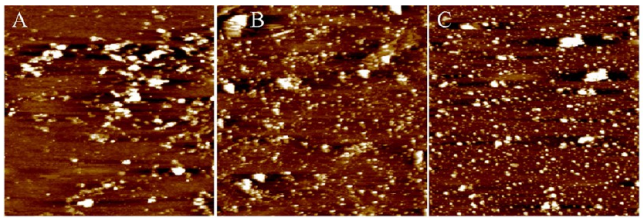

Figure 4. AFM images of 1 μM Aβ1−42 aggregates in the presence of heme at different concentrations: (A) 0.1, (B) 1, and (C) 10 μM. The samples were incubated at 37 °C for 24 h. The size of each AFM image is 2 μm × 2 μm.

Aβ by forming Aβ-heme complex, indicating that Aβ-heme complex could inhibit Aβ aggregation in vivo and dismantle aggregated Aβ.

Peroxidase Activity. The peroxidase activity of the Aβ1−42-heme complex and free heme was investigated by following the catalytic oxidation of the substrate of guaiacol in the presence of H_2O_2. The increase of the 470 nm absorbance intensity of oxidation product for the guaiacol was monitored by UV−vis absorbance spectra (Figure S3, Supporting Information), and the kinetic traces (Figure 5) were obtained.

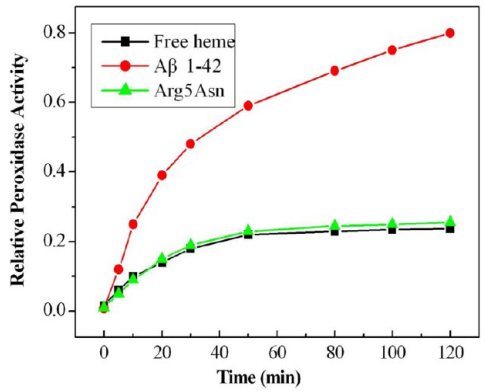

Figure 5. Kinetic traces for peroxidase activity of different heme-Aβ complexes: free heme, squares; Aβ1−42, circles; Arg5Asn, triangles.

Compared with the free heme, the Aβ1−42-heme complex showed obviously high peroxidase activity, demonstrating that the formation of histidine-bound complex had high peroxidase-like active site. The peroxidase activity of the Arg5Asn-heme complex was also determined because an acidic arginine residue existed in the distal side of heme and could provide the proton required for peroxidase activity.[21] Arg5Asn-Heme complex showed similar peroxidase activity to the free heme, demonstrating that Arg5 played an important role in making the Aβ1−42-heme complex as a peroxidase. Therefore, heme is able to bind heme, which not only inhibits Aβ aggregation but also catalyzes the decomposition of H_2O_2 and ROS due to the peroxidase activity of the Aβ-heme complex. Therefore, heme could protect neurons against Aβ cytotoxicity in vivo.[19,28]

CONCLUSIONS

In summary, the mechanism of Aβ-heme interaction has been elucidated by the use of electrochemical, morphological, and spectroscopic characterization. Our study indicates that (i) His13 and His14 residues could both bind heme under physiological conditions by forming an Aβ-heme complex, (ii) Aβ bound two molecules of heme, and the binding of the first heme molecule had higher affinity at lower concentration than the second heme molecule, and (iii) the combination of Aβ with heme inhibited the aggregation of Aβ and the Aβ-heme complex showed peroxidase activity. The results may provide insights into the role of heme on the ROS production and formation of Aβ fibrils and Aβ amorphous plaques in AD. Thus, our findings of interaction of Aβ and heme may provide insightful and valuable understanding of the AD pathogenesis.

METHODS

Materials. All peptides were obtained from ChinaPeptides Co., Ltd. (Shanghai, China) with >95% purity. For this study, wild-type Aβ1−42, Aβ1−16, Aβ1−16 site-directed mutants (His6Gly, His13Ala, His14Ala, Tyr10Gly, and Arg5Asn) were used. Hemin (which is referred to as heme in this paper) was purchased from Aladdin Reagent Ltd. (Shanghai, China). All other reagents were obtained from commercial suppliers and used without filtration. Pure water used was purified by using a Millipore M-Q purification system (>18 MΩ cm).

To obtain uniform, monomeric Aβ peptides, lyophilized peptides were dissolved to 2 mg mL^{-1} in 1,1,1,3,3,3-hexafluoroisopropanol (HFIP, Acros) and then incubated overnight at room temperature. HFIP was evaporated off by N_2 gas, and the peptide was redissolved in dimethyl sulfoxide (Sigma) to a concentration of 2 mM stored at −20 °C as stock solution. Heme stock solution was freshly prepared in 0.1 M NaOH to a concentration of 0.01 M and stored in the dark.

Electrochemical Measurements. A CHI820C electrochemical workstation (Shanghai Chenhua, China) was used for electrochemical analysis. All experiments were performed in a three-electrode cell system with glassy carbon (GC, 3 mm diameter), platinum wire, and saturated calomel electrode (SCE) as working electrode, auxiliary electrode, and reference electrode, respectively. Before use, the GC electrode was polished with aqueous slurries of fine alumina powders (1.0, 0.3, and 0.05 μm) on a polishing cloth and then sonicated in acetone and deionized water for 10 min in succession. In CV experiments, the scan rate was 20 mV s^{-1}. In DPV experiments, the amplitude was 0.05 V and the pulse width was 0.2 s. Unless otherwise stated, all experiments were carried out at room temperature in phosphate buffer solution (PBS, 0.1 M, pH 7.4). PBS was prepared using disodium hydrogen phosphate and potassium dihydrogen phosphate in deionzied water. The electrolyte solutions were purged with high-purity N_2 gas for 15 min to reduce the level of oxygen dissolved before each electrochemical measurement.

Determination of Binding Constant and Number of Binding Sites. Saturation binding experiments of heme with Aβ1−42 were carried out by the use of fixed concentration of Aβ1−42 (5 μM) and increasing concentrations of heme (1−20 μM). Scatchard plot were obtained in three steps. First, Aβ1−42 and heme were mixed in 0.1 M PBS (pH 7.4) and were incubated at 37 °C at dark for 1 h. Second, Aβ1−42 and Aβ1−42-heme were removed by high speed centrifugation (14 000 rpm for 5 min). Finally, the reduction peak current of unbound heme was measured by DPV measurements and then the concentration was read from the calibration curve of peak current versus concentration (Figure S1, Supporting Information).

Atomic Force Microscopy. AFM samples prepared in our previous work were used for this study.[29] First, freshly prepared Aβ1−42 or Aβ1−16 (1 μM) in a pH 7.4 PBS was incubated for 12 h at 37 °C. Second, the solid template (mica sheet) was adsorbed in nickel salt solution (10 mM) for 10 min and then rinsed twice with 200 μL deionized water. Finally, the above 10 μL peptide solution was deposited on the mica substrate, and then the sample was dried up by airing.

The morphology of Aβ1−42 in the presence or absence of heme was characterized by using an AFM instrument (Agilent 5500, Agilent Technologies). Each image was acquired in the tapping mode. All operations were done in an automated moisture control box with 30−40% humidity at room temperature.

Peroxidase Activity Measurement. Guaiacol was used as the substrate for peroxidase activity measurement.[30] The reaction mixture

dx.doi.org/10.1021/cn300231q | ACS Chem. Neurosci. 2013, 4, 535−539

(1 mL) contained 8 mM H_2O_2, 40 mM guaiacol, 50 mM sodium acetate buffer (pH 4.5), and 5 μM Aβ-heme complexes. Kinetic traces were obtained by monitoring the increase of the 470 nm absorption band with time on a UV 2300 spectrophotometer (Spain).

■ ASSOCIATED CONTENT

Supporting Information

(1) DPV of different concentration of heme, (2) calibration plots of the reduction peak current versus concentration of heme, (3) DPV of unbound heme, (4) concentration of the total heme, bound heme, and free heme, and (5) absorbance spectra before and after addition of the Aβ or mutants. This material is available free of charge via the Internet at http://pubs.acs.org.

■ AUTHOR INFORMATION

Corresponding Author

*E-mail: xumaotian@sqnc.edu.cn (M.X.); liult05@iccas.ac.cn (L.L.). Fax/Tel.: +86 370 2586802.

Author Contributions

Y.Z. and M.X. conceived methodology, analyzed the results, wrote the paper, and directed the project. J.W. and R.W. performed the experiments such as CV, DPV, AFM, and UV−vis spectroscopy. L.L. and X.L. critically reviewed and revised the manuscript.

Funding

The authors gratefully acknowledge the National Natural Science Foundation of China (Project Nos. 21105062, 21175091, and 21045003), Innovation Scientists and Technicians Troop Construction Projects of Henan Province, and Program for Innovative Research Team (in Science and Technology) in University of Henan Province for financial support.

Notes

The authors declare no competing financial interest.

■ REFERENCES

(1) Rauk, A. (2009) The chemistry of Alzheimer's disease. *Chem. Soc. Rev. 38*, 2698−2715.

(2) Kepp, K. P. (2012) Bioinorganic chemistry of Alzheimer's disease. *Chem. Rev. 112*, 5193−5239.

(3) Selkoe, D. J. (2001) Alzheimer's disease: genes, proteins, and therapy. *Phys. Rev. 81*, 741−766.

(4) Rauk, A. (2008) Why is the amyloid beta peptide of Alzheimer's disease neurotoxic? *Dalton Trans.*, 1273−1282.

(5) DeToma, A. S., Salamekh, S., Ramamoorthy, A., and Lim, M. H. (2012) Misfolded proteins in Alzheimer's disease and type II diabetes. *Chem. Soc. Rev. 41*, 608−621.

(6) Lemkul, J. A., and Bevan, D. R. (2012) The role of molecular simulations in the development of inhibitors of amyloid β-peptide aggregation for the treatment of Alzheimer's disease. *ACS Chem. Neurosci. 3*, 845−856.

(7) Hardy, J., and Selkoe, D. J. (2002) The amyloid hypothesis of Alzheimer's disease: progress and problems on the road to therapeutics. *Science 297*, 353−356.

(8) Clippingdale, A. B., Wade, J. D., and Barrow, C. J. (2001) The amyloid-β peptide and its role in Alzheimer's disease. *J. Pept. Sci. 7*, 227−249.

(9) Janus, C., Pearson, J., McLaurin, J., Mathews, P. M., Jiang, Y., Schmidt, S. D., Chishti, M. A., Horne, P., Heslin, D., French, J., Mount, H. T. J., Nixon, R. A., Mercken, M., Bergeron, C., Fraser, P. E., George-Hyslop, P. S., and Westaway, D. (2000) Aβ peptide immunization reduces behavioural impairment and plaques in a model of Alzheimer's disease. *Nature 408*, 979−982.

(10) Haass, C., and Strooper, B. D. (1999) The presenilins in Alzheimer's disease—proteolysis holds the key. *Science 286*, 916−919.

(11) Faller, P. (2009) Copper and zinc binding to amyloid-β: coordination, dynamics, aggregation, reactivity and metal-ion transfer. *ChemBioChem 10*, 2837−2845.

(12) Viles, J. H. (2012) Metal ions and amyloid fiber formation in neurodegenerative diseases. Copper, zinc and iron in Alzheimer's, Parkinson's and prion diseases. *Coord. Chem. Rev. 256*, 2271−2284.

(13) Miura, T., Suzuki, K., Kohata, N., and Takeuchi, H. (2000) Metal binding modes of Alzheimer's amyloid β-peptide in insoluble aggregates and soluble complexes. *Biochemistry 39*, 7024−7031.

(14) Bush, A. I. (2003) The metallobiology of Alzheimer's disease. *Trends Neurosci. 26*, 207−214.

(15) Barnham, K. J., and Bush, A. I. (2008) Metals in Alzheimer's and Parkinson's diseases. *Curr. Opin. Chem. Biol. 12*, 222−228.

(16) Howlett, D., Cutler, P., Heales, S., and Camiller, P. (1997) Hemin and related porphyrins inhibit β-amyloid aggregation. *FEBS Lett. 417*, 249−251.

(17) Atamna, H., and Frey, W. H., II. (2004) A role for heme in Alzheimer's disease: Heme binds amyloid β and has altered metabolism. *Proc. Natl. Acad. Sci. U.S.A. 101*, 11153−11158.

(18) Atamna, H., and Boyle, K. (2006) Amyloid-β peptide binds with heme to form a peroxidase: Relationship to the cytopathologies of Alzheimer's disease. *Proc. Natl. Acad. Sci. U.S.A. 103*, 3381−3386.

(19) Bao, Q., Luo, Y., Li, W., Sun, X., Zhu, C., Li, P., Huang, Z.-X., and Tan, X. (2011) The mechanism for heme to prevent Aβ1−40 aggregation and its cytotoxicity. *J. Biol. Inorg. Chem. 16*, 809−816.

(20) Atamna, H., Frey, W. H., II, and Ko, N. (2009) Human and rodent amyloid-β peptides differentially bind heme: Relevance to the human susceptibility to Alzheimer's disease. *Arch. Biochem. Biophys. 487*, 59−65.

(21) Pramanik, D., and Dey, S. G. (2011) Active site environment of heme-bound amyloid β peptide associated with Alzheimer's disease. *J. Am. Chem. Soc. 133*, 81−87.

(22) Santos, N. C., and Castanho, M. A.R.B. (2004) An overview of the biophysical applications of atomic force microscopy. *Biophys. Chem. 107*, 133−149.

(23) Ha, C., Ryu, J., and Park, C. B. (2007) Metal ions differentially influence the aggregation and deposition of Alzheimer's β-amyloid on a solid template. *Biochemistry 46*, 6118−6125.

(24) Jiang, D., Rauda, I., Han, S., Chen, S., and Zhou, F. (2012) Aggregation pathways of the amyloid β(1−42) peptide depend on its colloidal stability and ordered β-sheet stacking. *Langmuir 28*, 12711−12721.

(25) Lopes, P., and Kataky, R. (2012) Chiral interactions of the drug propranolol and α_1-acid-glycoprotein at a micro liquid-liquid interface. *Anal. Chem. 84*, 2299−2304.

(26) Xie, X., Wang, Z., Zhou, X., Wang, X., and Chen, X. (2011) Study on the interaction of phthalate esters to human serum albumin by steady-state and time-resolved fluorescence and circular dichroism spectroscopy. *J. Hazard. Mater. 192*, 1291−1298.

(27) Atamna, H. (2006) Heme binding to amyloid-β peptide: Mechanistic role in Alzheimer's disease. *J. Alzheimer's Dis. 10*, 255−266.

(28) Lloret, A., Badía, M.-C., Mora, N. J., Ortega, A., Pallardó, F. V., Alonso, M. D., Atamna, H., and Viña, J. (2008) Gender and age-dependent differences in the mitochondrial apoptogenic pathway in Alzheimer's disease. *Free Radical Biol. Med. 44*, 2019−2025.

(29) Zhou, Y. L., Huo, Z. H., Zhu, X., Zhu, X. H., Xu, M., and Liang, Y. (2012) Electrochemical monitoring of the interaction of Cu(II) with amyloid-β peptides on boron-doped diamond electrode. *Int. J. Electrochem. Sci. 7*, 3089−3101.

(30) Yuan, Z. Y., and Jiang, T. J. (2003) Horseradish peroxidase. In *Handbook of food enzymology* (Whitaker, J. R., Voragen, A., and Wong, D. W. S., Eds.), 1st ed., pp403−411, Marcel Dekker Inc., New York.